NASA Technical Memorandum

NASA TM-86554

A DIGITAL IMAGING PHOTOMETRY SYSTEM FOR COMETARY DATA ACQUISITION

Center Director's Discretionary Fund Final Report

By K. S. Clifton, C. M. Benson, and G. A. Gary

Space Science Laboratory
Science and Engineering Directorate

July 1986

(NASA-TM-86554) A DIGITAL IMAGING PHOTOMETRY SYSTEM FOR COMETARY DATA ACQUISITION Center Director's Discretionary Fund Final Report (NASA) 28 p CSCL 03A

N86-32373

Unclas

G3/89 43102

National Aeronautics and Space Administration

George C. Marshall Space Flight Center

TECHNICAL REPORT STANDARD TITLE PAGE

1. REPORT NO.	2. GOVERNMENT ACCESSION NO.	3. RECIPIENT'S CATALOG NO.
NASA TM-86554		

4. TITLE AND SUBTITLE	5. REPORT DATE
A Digital Imaging Photometry System for Cometary Data Acquisition — Center Director's Discretionary Fund Final Report	July 1986
	6. PERFORMING ORGANIZATION CODE
7. AUTHOR(S) K. S. Clifton, C. M. Benson, and G. A. Gary	8. PERFORMING ORGANIZATION REPORT #
9. PERFORMING ORGANIZATION NAME AND ADDRESS George C. Marshall Space Flight Center Marshall Space Flight Center, Alabama 35812	10. WORK UNIT NO.
	11. CONTRACT OR GRANT NO.
12. SPONSORING AGENCY NAME AND ADDRESS National Aeronautics and Space Administration Washington, D.C. 20546	13. TYPE OF REPORT & PERIOD COVERED Technical Memorandum
	14. SPONSORING AGENCY CODE

15. SUPPLEMENTARY NOTES

Prepared by Space Science Laboratory, Science and Engineering Directorate.

16. ABSTRACT

This report describes a digital imaging photometry system developed in the Space Science Laboratory at the Marshall Space Flight Center as part of the Center Director's Discretionary Fund (CDDF). The photometric system used for cometary data acquisition is based on an intensified secondary electron conduction (ISEC) vidicon coupled to a versatile data acquisition system which allows real-time interactive operation. Field tests on the Orion and Rosette nebulas indicate a limiting magnitude of approximately $m_V = 14$ over the 40 arcmin field-of-view. Observations were conducted of Comet Giacobini-Zinner in August 1985. The resulting data are discussed in relation to the capabilities of the digital analysis system. The development program concluded on August 31, 1985.

17. KEY WORDS	18. DISTRIBUTION STATEMENT
Digital Image Photometer, Comets, SEC Vidicon	Unclassified — Unlimited

19. SECURITY CLASSIF. (of this report)	20. SECURITY CLASSIF. (of this page)	21. NO. OF PAGES	22. PRICE
Unclassified	Unclassified	27	NTIS

MSFC - Form 3292 (May 1969)

For sale by National Technical Information Service, Springfield, Virginia 22151

TABLE OF CONTENTS

LIST OF ILLUSTRATIONS

TECHNICAL MEMORANDUM

DIGITAL IMAGING PHOTOMETRY SYSTEM FOR COMETARY DATA ACQUISITION

Center Director's Discretionary Fund Final Report

I. INTRODUCTION

With the increased interest in cometary observations of recent years, brought about in part by the 1985-1986 apparition of Comet Halley, many different types of imaging systems are being utilized to obtain scientific data on these objects. This report describes one of these systems, a digital imaging photometer, developed at the Marshall Space Flight Center (MSFC).

Comets are among the most primitive bodies in the solar system. They have suffered little alteration from sources such as solar irradiation, since most of their existence is spent in the Oort cloud of the outer regions of the solar system. Since they are small, comets have also not been significantly modified by internal processes. Therefore, they have retained the chemical and physical characteristics of the original material from which they, and the solar system, were formed. This makes the study of comets in general a key part in the efforts to understand the formation and evolution of the solar system. In addition, knowledge resulting from cometary studies may also aid in the understanding of the formation and nature of interstellar dust clouds and dark nebulae, due to the potential similarities in the composition of these objects.

With the current apparition of Halley's Comet, a number of ground-based and space-borne observations are being conducted to investigate this comet in visual and extended wavelengths. Included in these observations are infrared measurements conducted by the Space Science Laboratory of MSFC using a bolometer infrared detector array. From these observations, it has become apparent that an optical adjunct to the infrared measurements would enhance the data by making simultaneous measurements in the visual wavelength regions. For maximum utility, it would also be desirable for this optical system to be portable, easily interfaced to large or small telescopes, capable of real-time playback in addition to long-term data storage, and suitable for real-time analysis and adjustment in order to better portray features of interest.

With these characteristics in mind, a system was conceived not only for use as an adjunct to infrared measurements but also fully capable of obtaining data with intrinsic scientific merit [1]. Such an instrument could help to provide much needed information required to resolve important questions identified by the cometary science community, such as what are the parent molecules for the various radicals observed in comets and why does the variation in cometary brightness with heliocentric distances not follow the theoretically predicted form? Concerning this latter problem, the evaporation rate of gases from the nucleus is determined by the amount of heat supplied by the Sun, which varies as the inverse square of the heliocentric distance. In addition, the photodissociation and fluorescence mechanisms each obey an inverse square law implying that the total variation should be to the inverse sixth power. Observations confirm this for some species (e.g., H OH, CH, NH), but the data for C_2 and C_3 suggest an inverse third or fourth-power dependence [2,3]. The poor

quality of the data for other radicals leads to considerable uncertainty. Also, the lack of data at large heliocentric distances leaves much to be done toward determining the parent molecules for the various radicals as well as the processes affecting the comet during its apparition. An imaging photometer with a high quantum efficiency allows the study of cometary photochemistry and molecular production rates at greater heliocentric distances than would otherwise be possible. A high quantum efficiency also provides greater temporal resolution permitting the determination of the rotational periods of comets by techniques previously used in such observations [4]. In addition, the imaging capability of the detector will allow the study of morphological variations of a comet throughout its apparition, including a study of cometary mass motions. Finally, the chemical coma size varies with the spectral emission and an imaging system is required to obtain the extended emission for appropriate data interpretation.

II. INSTRUMENT CONCEPT

The observation of faint, distant comets requires the ability to detect a very low flux of light, whereas accurate photometry requires a relatively high signal-to-noise ratio. Past efforts to improve the signal-to-noise ratio have been concentrated on integrating the light on the detector itself, or coherently adding low signal-to-noise measurements. The approach used with the digital cometary photometer is a combination of these in which an integrating detector is utilized in conjunction with an image processor to average incoming signals. A schematic of the overall field system is shown in Figure 1. Essentially, the system consists of an imaging detector and a low-light-level television camera with high quantum efficiency, adapted to a telescope. The output signal of the camera is delivered to a processor where it is digitized and temporarily stored for data manipulation and reduction. Real-time reduction of data is accomplished under computer control and stored on disc memory for later retrieval and further analysis.

A. Imaging Detector

The imaging detector consists of a low-light-level Secondary Electron Conduction (SEC) vidicon fiber-optically coupled to a single-stage intensifier. Operational specifics of the SEC vidicon are reported elsewhere [5,6]. The intensified SEC vidicon (ISEC) camera tube possesses the high sensitivity required to image faint sources as well as the capability to integrate weak signals over relatively long periods of time. The system also possesses high resolution and a comparative lack of capacitive lag. For these reasons the SEC vidicon has been employed in a wide variety of astronomical observations [7,8]. Although the ISEC camera generally displays less gain and dynamic range than an intensified silicon intensified target (ISIT) camera, it also exhibits less dark current and is more suited for performing integration of target signals. In addition, the noise structure is considered to be finer, and there is no evidence for ions or scintillations in the resulting image.

A camera tube utilizing a 40-mm photocathode with a S-20 extended red spectral response was utilized for the detector. With a sensor gain of up to 3.5×10^6, the sensitivity of the camera to 2854 K light is sufficient to produce 200 TV lines at 1.2×10^{-7} fc. The camera system operates with a 525-line interlaced TV raster at the normal television frame rate of 30 frames/s. Whereas the camera head contains the

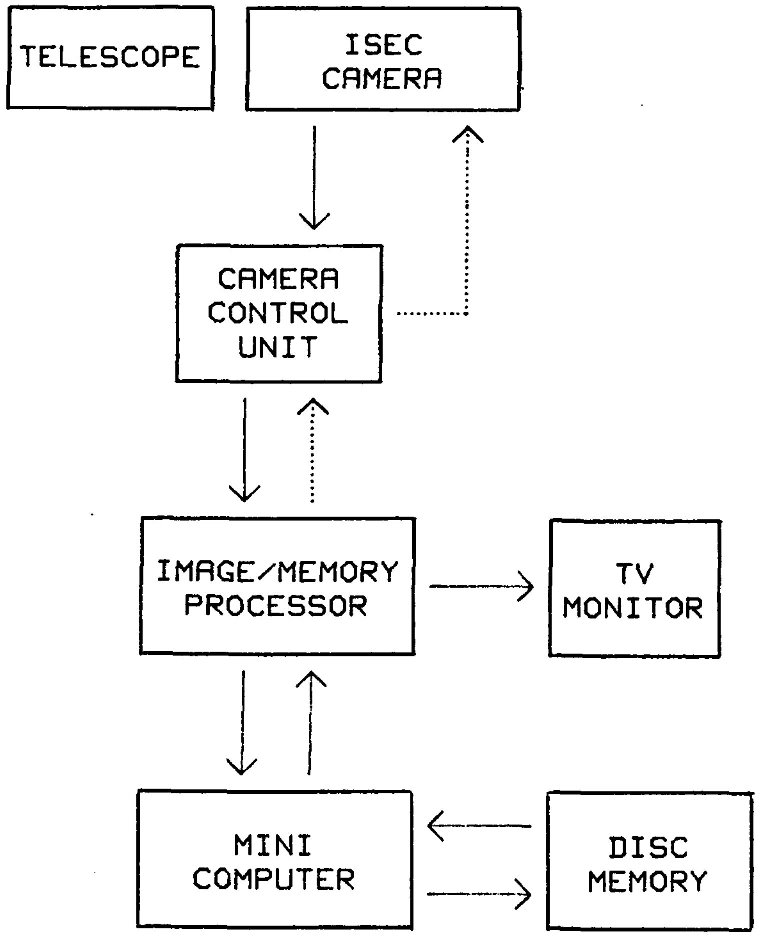

Figure 1. Schematic representation of the digital cometary photometric imager.

image detection components, the camera-control unit contains circuitry for video processing and control. Adjustable controls on the camera control unit include the gain of the video amplifier; the potential gain on the intensifier and camera tube, hence, signal gain; the amount of scanning beam current that affects resolution; and the focus of the scanning beam. The video gain is normally kept at a low value to maximize the signal-to-noise ratio of the resulting image.

B. Memory Processor

The analog signal from the camera is routed to an image/memory processor where it is digitized and stored. The memory processor combines a fast A/D converter, a high capacity random access memory, and a high-speed arithmetic unit, all under microprocessor control. The unit possesses a high-speed digitizing capability of 10 MHz and operates with a dynamic range of 8 bits per picture element (pixel) yielding a grayscale range of 0 to 255. Complete video frames composed of a 512 x 512 pixel format are stored in memory within 1/30 second. A frame grabbing

capability when initiated holds the next input image in memory for prolonged display on a TV monitor. Arithmetic functions allow the selective summation and subtraction of consecutive frames. In addition, any number of successive images (<100) may be averaged, thus increasing the image signal-to-noise ratio. Adjustable controls for the A/D limits are used to establish the desired contrast in an image between the black and white levels. An integrated control interfaced to the camera control unit determines the length of signal integration by the camera tube. Other features of the processor include a selectable output transform, which allows the differential gain of the input/output curve to be varied in any of three amplitude ranges, and an auto-sequencer which allows a complex sequence of processor operations to be performed, both automatically and repeatedly. These and other operations may be accomplished by the processing of stored data either with the internal microprocessor of the unit or with an external computer given direct access to the stored data by means of a random access input/output post. Independent of any other operation, the unit continuously displays its current memory state on standard TV monitors.

C. Minicomputer

A portable microcomputer used in the field to reduce and analyze image data possesses a storage capacity of 768 K-bytes of memory and utilizes an 8 M-byte Motorola MC 68000 microprocessor. Program information and relevant graphics are portrayed on a monochromatic 400 x 300 pixel display. External connection to the image/memory processor is made through an IEEE-488 interface. The computer also utilizes a 4 M-byte hard disc with a 270 K-byte micro-floppy drive for program and data storage. Twelve separate images with a 512 x 512 pixel format can be stored on the hard disc at one time. As an alternative, the disc can also store a higher number of images with reduced resolution, e.g., 48 images with a 256 x 256 pixel format. In addition, data can also be stored on individual micro-floppy discs at the rate of one 512 x 512 image per disc.

The basic configuration of the observational and data acquisition system are shown in Figures 2a-b. Figure 2a displays the camera fitted to a small 8-in. (20 cm) folded-optical telescope. The focal length of the f/10 Cassegranian system is approximately 2000 mm. A special adapter plate was designed and constructed to mount the camera and telescope to a telescope equatorial drive unit. A small finder scope can also be seen in the figure attached to the telescope. Figure 2b shows the field data acquisition system composed of the camera control unit, image/memory processor, minicomputer, and video monitor.

III. FIELD SYSTEM SOFTWARE

System software for field use was designed for image storage and retrieval as well as real-time data reduction and analyses. The Cometary Data Acquisition Processing System (CDAPS) provides the operator with an interactive basis for processing observational data. The basic functions of the program include image transfer, pixel data readout, image analysis, and celestial coordinate determination. A sample CDAPS menu is shown in Figure 3.

As seen from Figure 3, image transfer may be accomplished in any one of three ways.

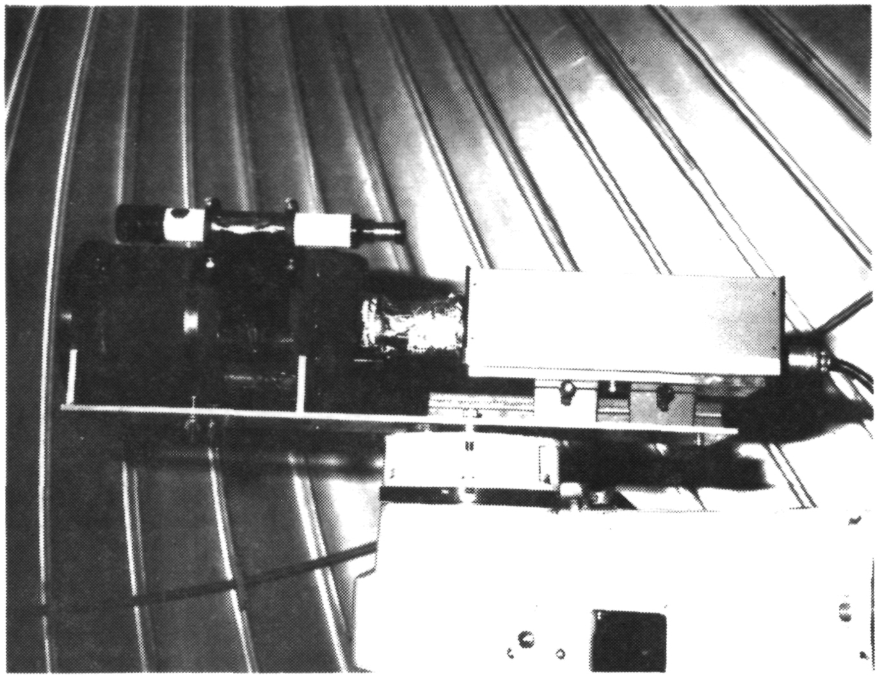

(a)

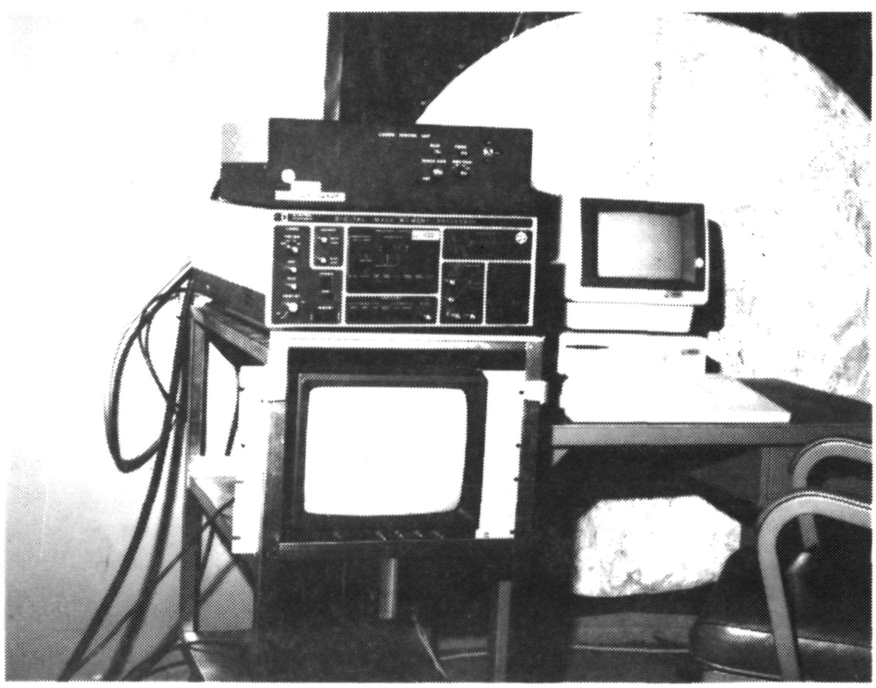

(b)

Figure 2. (a) View of the observational equipment, an ISEC vidicon attached to an 8-in. (20 cm) telescope, used to obtain cometary data. The system is mounted to an equatorial drive at a MSFC observatory. (b) View of the data acquisition system used to process the ISEC vidicon signal.

```
                    Cometary Data Acquistion Processing System      Revision 2.0

CDAPS Command Menu; Select option from the list below
(0)  Image Cursor Routine
(1)  Transfer Image   DS-20 Image Processor -->> 9133A Disc Memory
(2)  Transfer Image   9133A Disc Memory     -->> DS-20 Image Processor
(3)  Transfer Image   9133A Disc Memory     -->> Tape Drive 1
(4)  Image Line Contour Routine
(5)  Multiple Line Average and Plot Routine
(6)  Image Grayscale Contour Routine

        Celestial Object                    Hour Angle         Declination
1) COMET GIACOBINI-ZINNER                  - 0h 18m 26s          +48.50
2) BETA ORIONIS                            - 1h 22m 39s          - 8.25
3) GAMMA ERIDANUS                          - 0h 05m 43s          -13.65
4) BETA FORNAX                             + 1h 04m 15s          -32.62

Press numeric key (0-6) to make selection from menu above

  Object #1     |Object #2     |SET TIMEDATE  |Sidereal time |
  Object #3     |Object #4     | 04:35:55 CDT | + 3h 50m 04s |
```

Figure 3. Command menu of the Cometary Data Acquisition Processing System (CDAPS).

Option (1): The image appearing in the image processor may be stored in disc memory. When initiated, this option displays a listing of images currently stored in memory, a sample of which is shown in Figure 4. The listing provides file number, the time (local) and date that the image was obtained, the camera integration time, and the subject of the observation annotated with any additional desired information. Any image in memory can be replaced with a new image by proper file selection.

Option (2): Any image stored in disc memory can be transferred to the image processor for viewing or for data reduction and analysis. When initiated, this option also displays the listing of images stored in memory as with option (1).

Option (3): Any image stored in disc memory can be transferred to 9-track digital tape for permanent data storage and further data analysis.

The pixel data readout function [option (0)] allows the x-y position and grayscale of any picture element to be displayed on the computer terminal. A blinking cursor can be positioned manually to any point on an image displayed by the image/memory processor. The speed of cursor movement across the image is manually selectable to four values. When positioned, the option displays not only the desired pixel values but similar values for a block of 7 x 13 pixels centered about the cursor, as shown for a stellar image in Figure 5a. In addition, the average grayscale value of the pixel block is displayed as is the standard deviation of grayscale values.

Interactive CDAPS
Current Image Directory

	Time of Recording	Integration Time	Image Description
1	04:14:42 22 Aug 1985	60	COMET GZ NO AVG
2	04:18:24 22 Aug 1985	80	COMET GZ 4 FRM AVG
3	02:20:39 22 Aug 1985	30	COMET GZ NO AVG * 4h 34m RA 48.5 DEC
4	02:32:44 22 Aug 1985	30	COMET GZ 4 AVG * 4h 21m RA 48.5 DEC
5	02:38:51 22 Aug 1985	30	COMET GZ NO AVG
6	03:02:35 22 Aug 1985	50	COMET GZ 4 FRM AVG
7	03:12:34 22 Aug 1985	38	COMET GZ NO AVG HIGH CONTRAST
8	03:24:14 22 Aug 1985	30	COMET GZ 4 FRM AVG
9	03:32:12 22 Aug 1985	30	COMET GZ NO AVG
10	03:40:29 22 Aug 1985	30	COMET GZ 32 FRM AVG
11	03:54:06 22 Aug 1985	60	COMET GZ 8 FRM AVG
12	04:13:15 22 Aug 1985	60	COMET GZ 8 FRM AVG

Figure 4. Sample current image directory stored by CDAPS.

The data processing capabilities of CDAPS include contouring and the generation of intensity line scans. From Figure 3 these capabilities are:

Option (4): Image line contouring can be accomplished over a selectable 32 x 32 pixel area centered about coordinates input from computer keyboard or through the use of the cursor subprogram as in option (0) above. The desired maximum and minimum contour grayscale levels are input into the computer from which a set of contour intervals are calculated and drawn on the computer graphics display. A set of 10 contour intervals are generated with a step size determined automatically from these maximum and minimum values. An example of the contour output for a stellar image is shown in Figure 5b.

Option (5): Image grayscale contouring is achieved over a 32 x 32 pixel area similar to that in option (4). In this mode the computer generates 16 contour intervals with equal step sizes dependent upon the maximum and minimum grayscale values input by the user. The image is then graphically reproduced with a set of 16 different dot patterns corresponding to the contour intervals as shown in Figure 5c for the identical image used in Figure 5b.

Option (6): Image line scans portray the variation of image intensity with position along a line between two selectable endpoints. The intensity scale is determined automatically from the maximum and minimum grayscale values encountered along the line. Plots can be generated along either the x- or y-axis depending upon the slope of the desired scan. Multiline averages can also be determined with the same technique. The image line scan is demonstrated in Figure 5d.

The celestial coordinate determination function of CDAPS is directed more toward observational mechanics than data reduction or analyses. The program generates the position (hour angle) of up to four astronomical targets simultaneously as illustrated toward the bottom of Figure 3. Accurate positions are displayed on a continuous

Row\Col		261	262	263	264	265	266	267	268	269	270	271	272	273
298	-	10	15	13	12	22	36	40	32	29	19	19	18	20
299	-	15	19	17	16	35	87	95	64	43	24	22	21	19
300	-	13	15	20	19	64	146	167	126	74	44	27	20	23
301	-	19	15	19	23	71	164	200	166	94	49	26	13	15
302	-	18	15	25	27	60	138	178	138	80	47	28	20	18
303	-	17	18	23	31	35	95	138	105	65	38	25	18	20
304	-	25	22	26	30	35	52	77	66	45	30	24	24	21
305	-	18	23	31	32	34	42	50	42	26	19	15	11	14
306	-	18	19	22	29	34	36	37	33	24	20	16	12	15

Average = 42.5 Standard Deviation = 40.72

Figure 5a

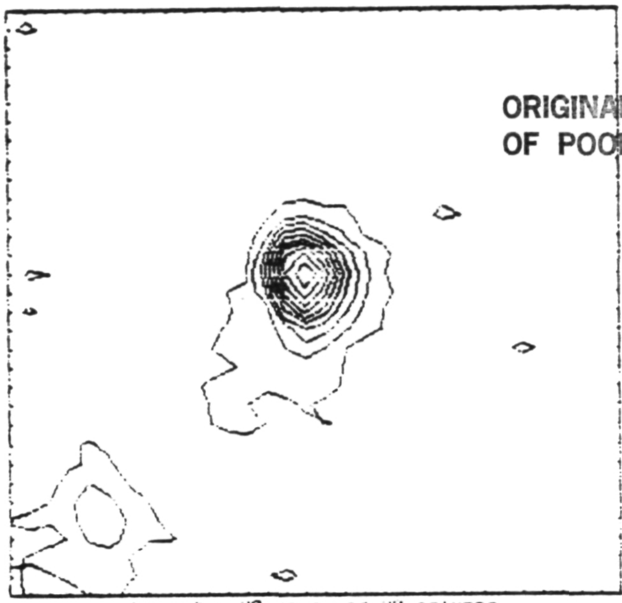

Array has 32 rows and 32 columns.
Minimum: 25; Maximum: 200; Contour interval: 17.5.

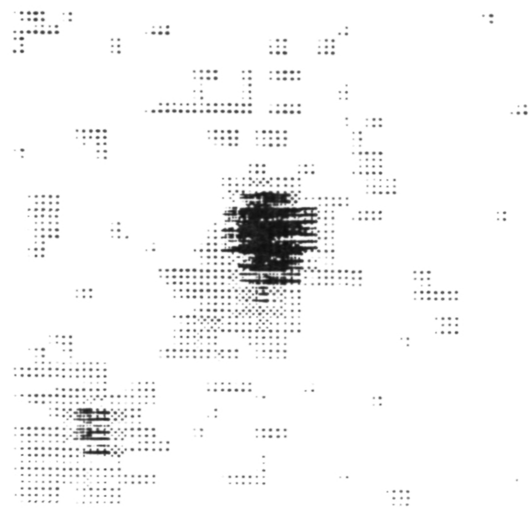

- Figure 5c

Figure 5b

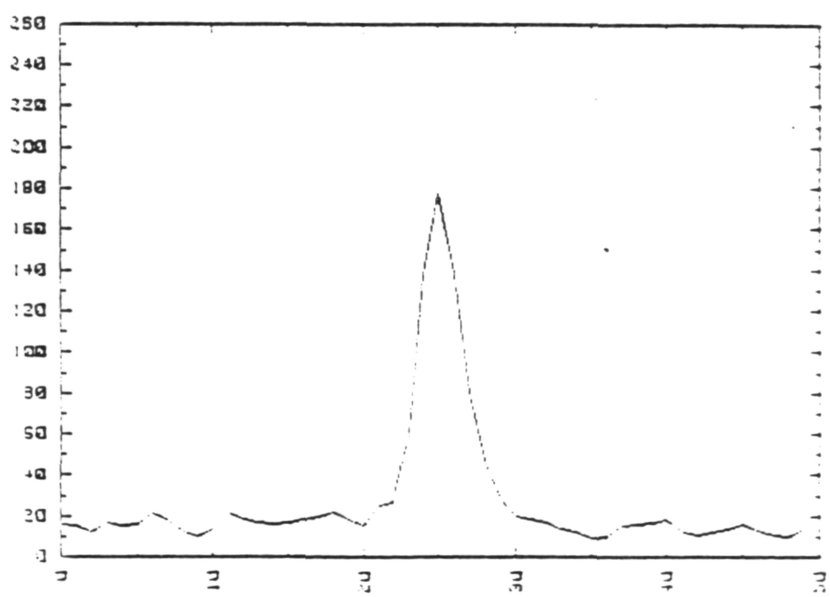

Figure 5d

Figure 5. (a) Digital representation of a star as processed by CDAPS from video data. (b) A CDAPS line contour of the same star. (c) A CDAPS graphic contour of the star. (d) A CDAPS line scan across the star with the ordinate given in grayscale intensities and the abscissa in pixel position.

basis, with the values updated each second. To attain these results, the user is required to input the right ascension and declination of each designated target in addition to a single input of the time and date. The program facilitates the procedures for telescope pointing using the observatory equatorial mount.

IV. VIDEO IMAGE PROCESSING SYSTEM (VIPS)

While observational data are obtained and stored, and to some extent analyzed by the cometary imaging system described previously, the bulk of the analysis is accomplished using the laboratory-based Video Image Processing System (VIPS) at the Space Science Laboratory of MSFC. A limited discussion of the VIPS is presented here because of its integral involvement with the cometary data analysis.

A schematic representation of the VIPS and its interfaces with the cometary imaging system is shown in Figure 6. The core of the system is a colorgraphics computer with a 2 M-byte RAM memory and a 9.8 M-byte Winchester disc. The color graphics capability provides a 512 x 390 pixel image in as many as 16 colors. Digital data from the disc storage unit of the digital cometary photometer may be transferred to 9-track digital tape and from tape to the VIPS hard disc memory for permanent storage. The VIPS disc memory is capable of storing approximately 250 images of 512 x 512 pixel format. The data can be recalled from tape or disc memory and displayed on one of two image/memory processors and associated video monitors. A graphics tablet used in conjunction with the computer provides remote user interaction with the VIPS by allowing the user to select program options by means of a stylus. Numerical data output may be read from the computer CRT or an impact printer which provides hard copies of the image in digital format. Color contours can be displayed on the CRT or by means of an 8-pen sheet-fed plotter. The computer and accessory units are connected through IEEE-488 interface buses.

V. SYSTEM PERFORMANCE

Following extensive in-house operational tests, the digital cometary photometer was taken to the field for observation of astronomical targets. Extended objects more typical of cometary phenomena, such as the Orion and Rosette nebulas, were viewed to demonstrate the system and its performance. The Orion nebula, in particular, afforded an excellent subject with a broad dynamic range of brightness, varying from a bright central region to faint filamentary structure at the outer edges; all of this concentrated within the 40 arcmin diameter field-of-view of the detector. Figure 7a is a representative view of the Orion nebula (right ascension - 5^h32^m; declination = -5.4 deg) obtained with the system on the evening of April 10, 1985, at 19^h50^m local time. The view is an average of four consecutive images each with an integration time of 0.47 s (14 video frames). The final image was obtained in approximately 2 s.

Figure 7b portrays the starfield corresponding to the image of Figure 7a. Visual magnitudes obtained from the Smithsonian Astrophysical Observatory Star Catalog [9] and Burnham's Celestial Handbook [10] are also shown in the figure. A threshold magnitude for the image of approximately $m_v = 14$ is based on the observation that stars fainter than $m_v = 13$ are clearly discernible. The distortion of some

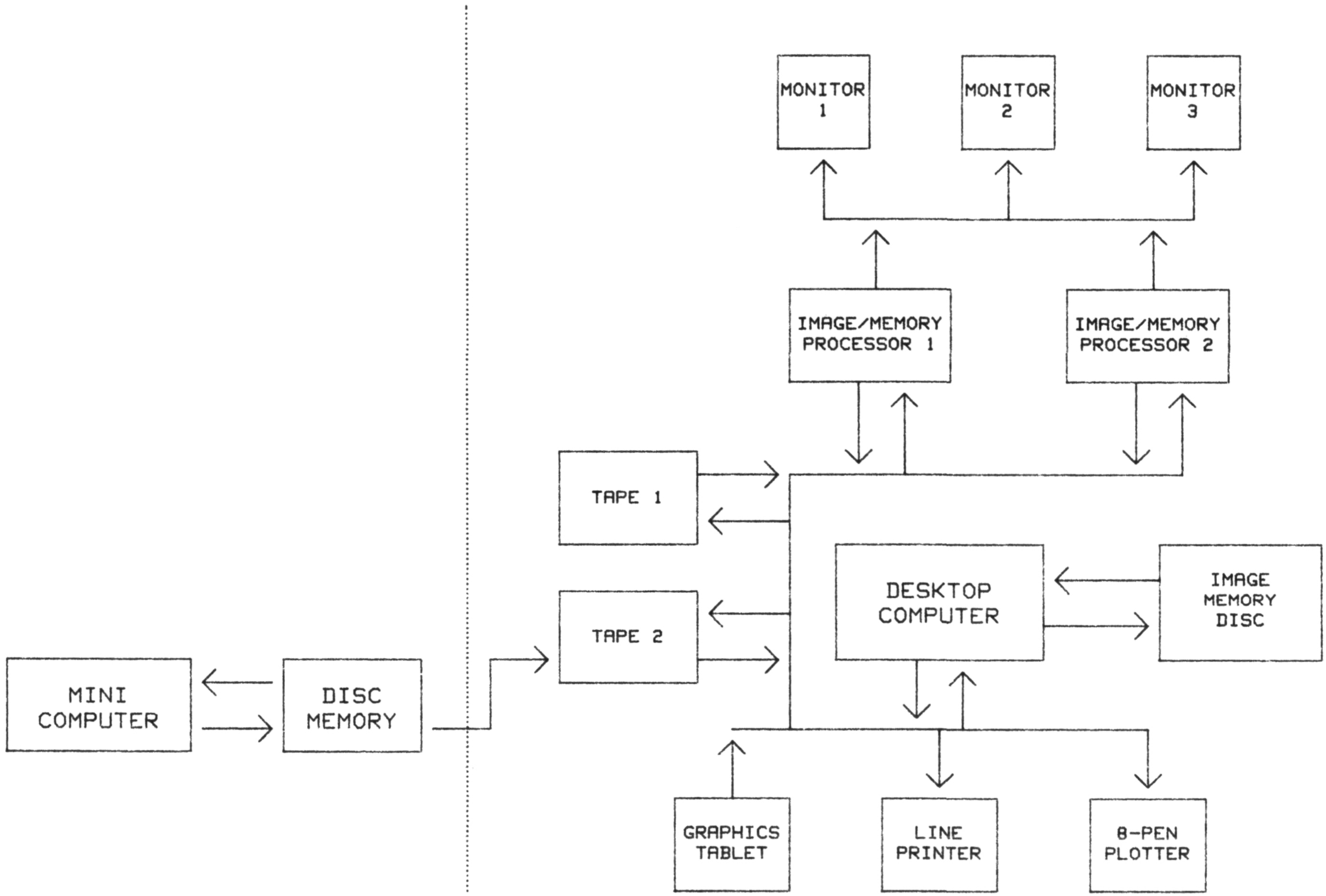

Figure 6. Schematic representation of the VIPS used for data analyses.

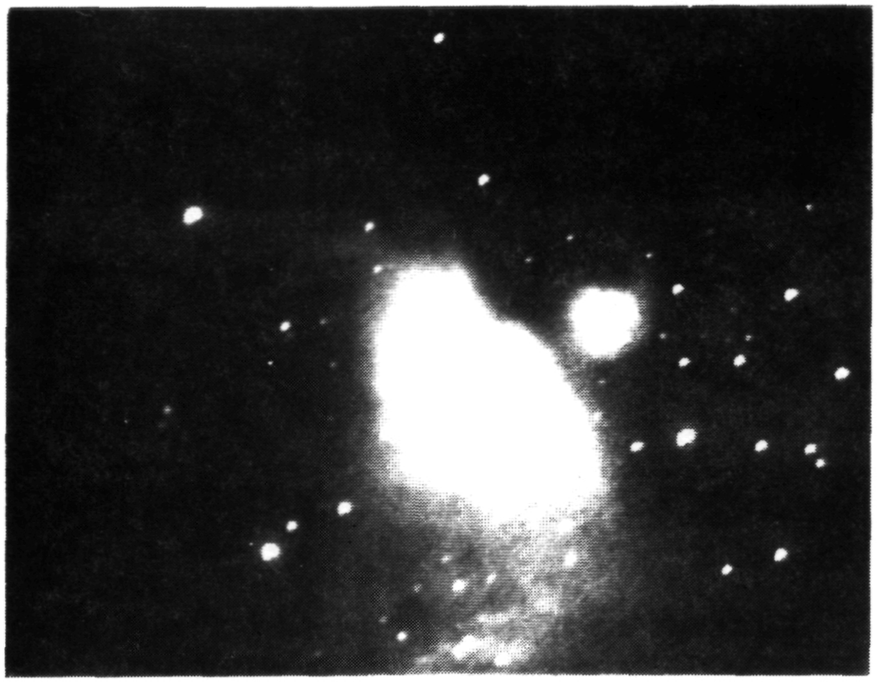

(a)

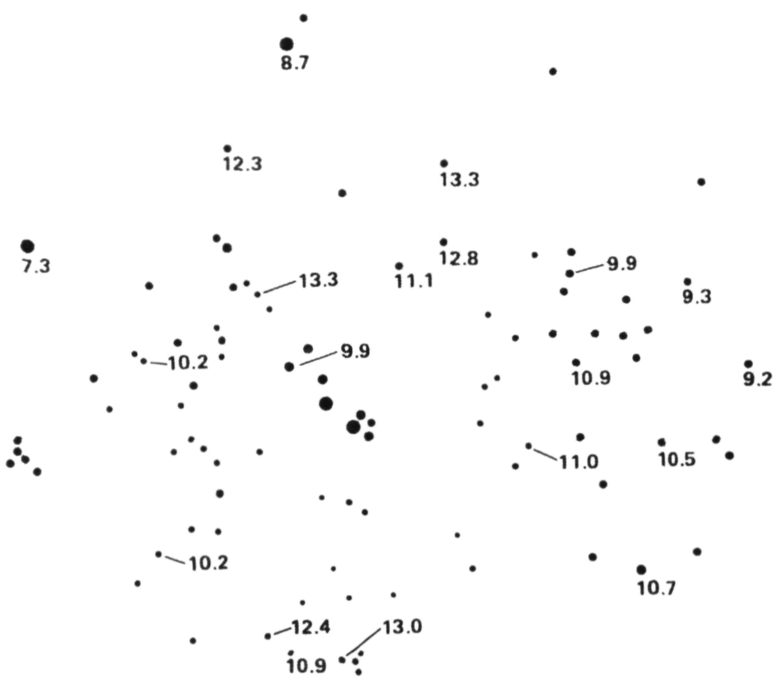

(b)

Figure 7. (a) View of the Orion nebula as obtained in four averaged frames each integrated for 0.47 s with the digital cometary photometric imager. (b) Starfield corresponding to the view of Figure 7a. Comparison magnitudes are given for selected stars.

of the brighter stellar images is due to imperfect optics and a slight motion of the sky with respect to the telescope drive.

The effect of increased camera integration times may be noted from Figures 8a-d, which illustrate the same field-of-view obtained with integrations of 0.03, 0.13, 0.23, and 0.33 s (1, 4, 7, and 10 video frames), respectively. It is apparent from this series that, due to limitations in the dynamic range of the ISEC camera tube, a range of integrations may be necessary to study both the brighter and fainter regions of an extended object such as a comet with a bright coma and faint tail structure.

Figure 9 illustrates the effect of increased integration time on the images of various stars with respect to total brightness. This total brightness is determined from the summation of differences in pixel grayscales and background values within the perimeter of the star image. With lengthened exposure time, not only are the stellar grayscale values increased, but the perimeter of the identifiable star boundary is enlarged significantly. As the image approaches saturation, nearly all of the increase in brightness is reflected in the physical growth of the image. At these levels the system displays a pronounced nonlinear response function. Whereas these nonlinearities set upper limits to useful photometric studies at longer integrations (or for bright objects), A/D level settings (contrast) of the camera can limit the system at short integrations by establishing the detection threshold level above the general noise background. In this case the background pixels register values of zero, and stellar images have correspondingly reduced grayscale values. For these reasons, the stars shown in the study of Figure 9 were selected to be in the magnitude range of m_V = +10 to +11. It should be emphasized that the curves shown in Figure 9 are illustrative only of the basic trend caused by increasing the integration time, since changing the camera A/D levels or gains will result in curves of different slopes. As long as brightness calibrations can be conducted using known starfield images, this presents only a slight problem.

In order to conduct more accurate photometric analyses for a wider dynamic range of brightness, a means is being developed to compensate for the incomplete image readout of the camera target by a single scan of the electron neutralizing beam. Modifications of the camera system are currently underway to permit a designated reduction of the intensifier high voltage, thus effectively halting the accumulation of additional signal by inhibiting charge buildup on the camera target. Successive image scans will be stored, summed, and normalized to produce an image with greater photometric accuracy, particularly for brighter objects.

The effect of averaging successive frames is shown in Figures 10a-b where both averaged and unaveraged views of a section of the Rosette nebula are compared. The field-of-view is centered at right ascension = $6^h 29^m$; declination = 5.2 deg. The faint variations of brightness throughout the fields-of-view are a real effect due to the structure of the nebula which is larger than the field-of-view of the camera. The brightness of these structures are near the detection threshold of the system as viewed on the evening of April 10, 1985. The exception to this is the dark vertical bar in the left center of the image due to a system artifact. Figure 10a shows the unaveraged data of a single frame, while Figure 10b shows the result of averaging 16 consecutive frames. Samples of digital grayscale values indicate that the 16-frame average reduces the standard deviation of the background noise from 25 percent of the average noise level to 8 percent. Some image smear may be apparent with longer frame averages, particularly if any image motion is discernible.

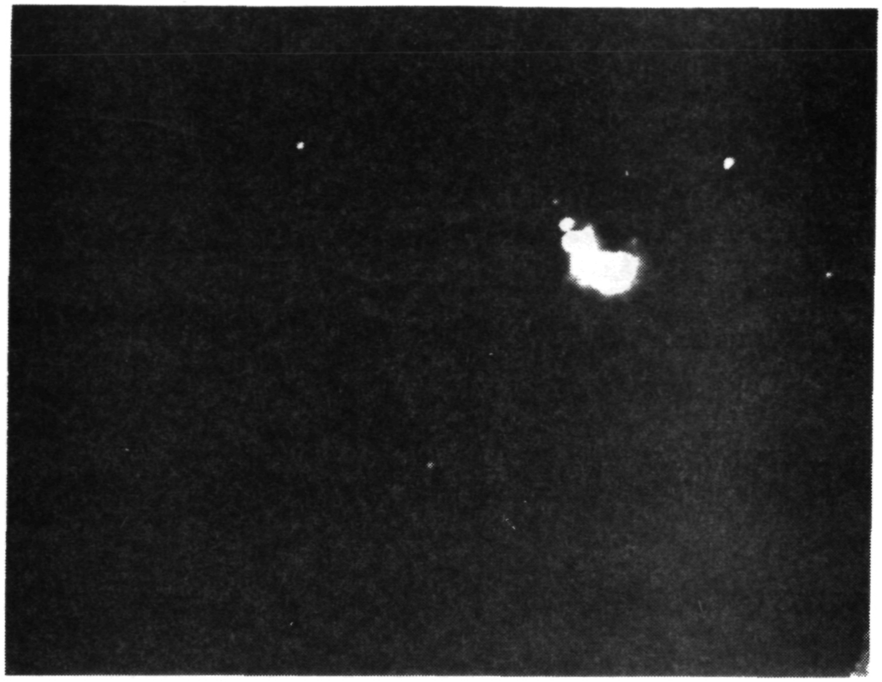

(a)

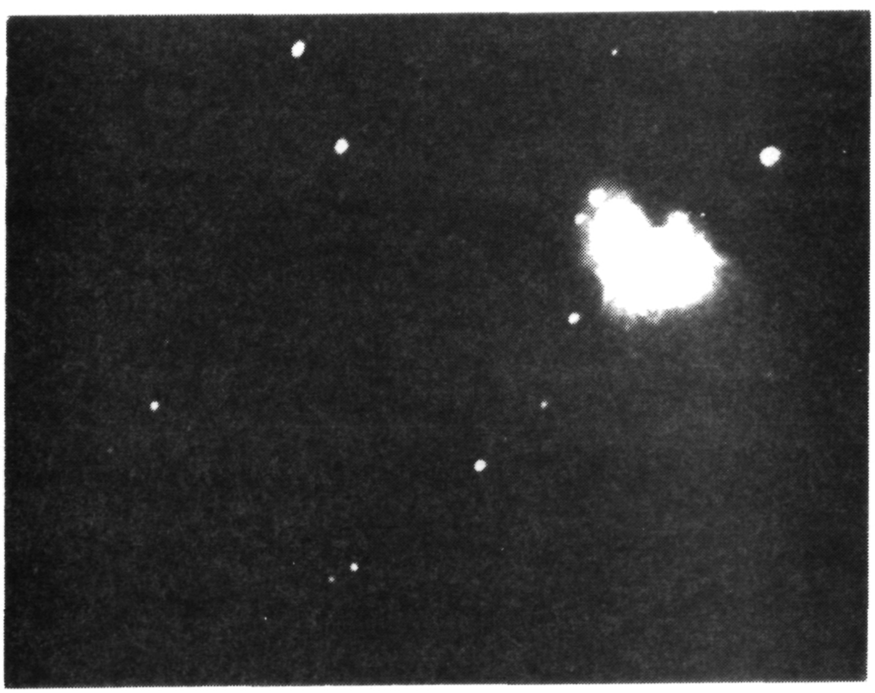

(b)

Figure 8. A view of the Orion nebula obtained with a (a) 0.03 s exposure, (b) 0.13 s exposure, (c) 0.23 s exposure, and (d) 0.33 s exposure.

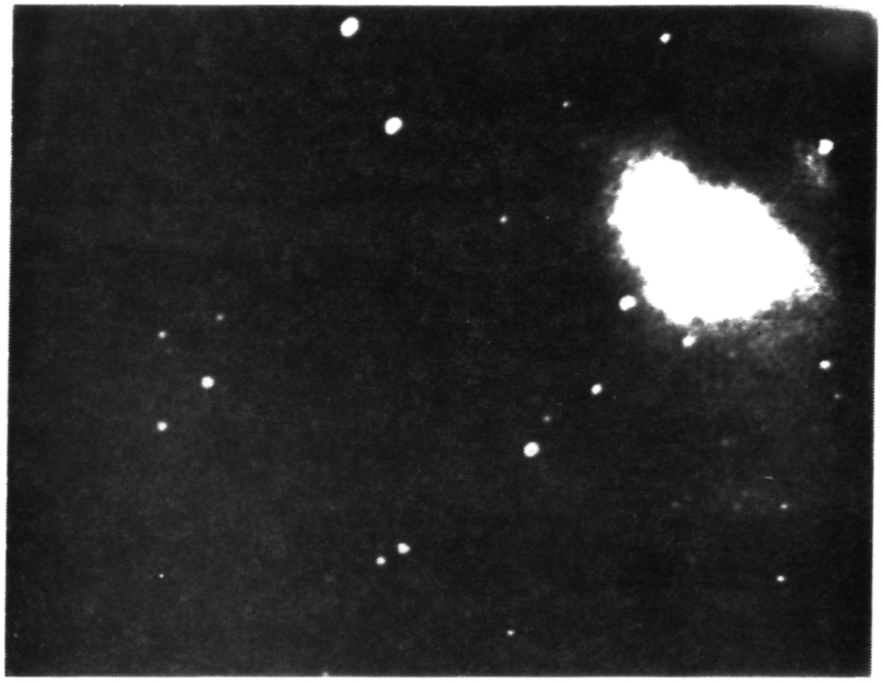

(c)

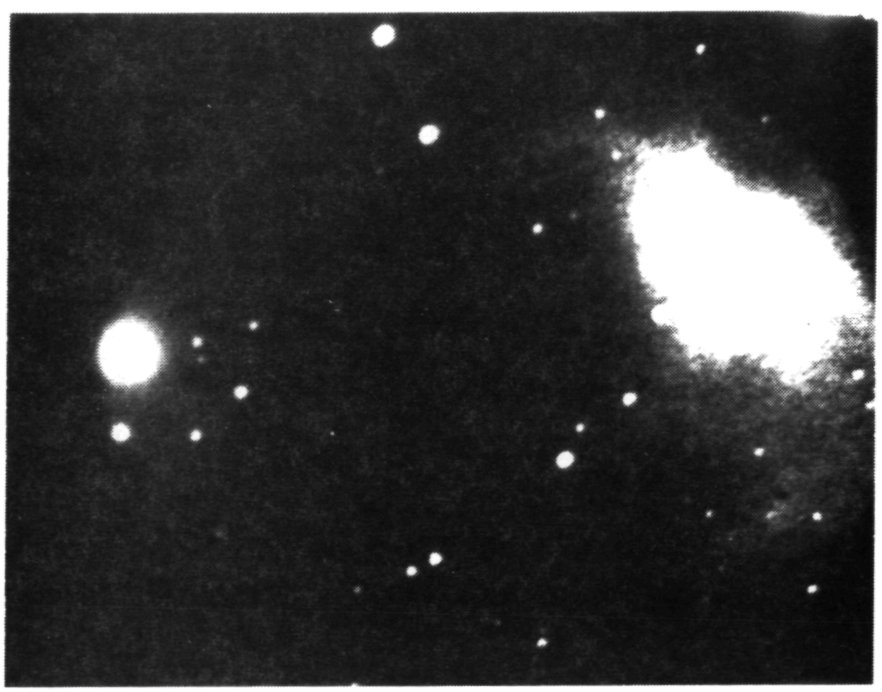

(d)

Figure 8. (Concluded).

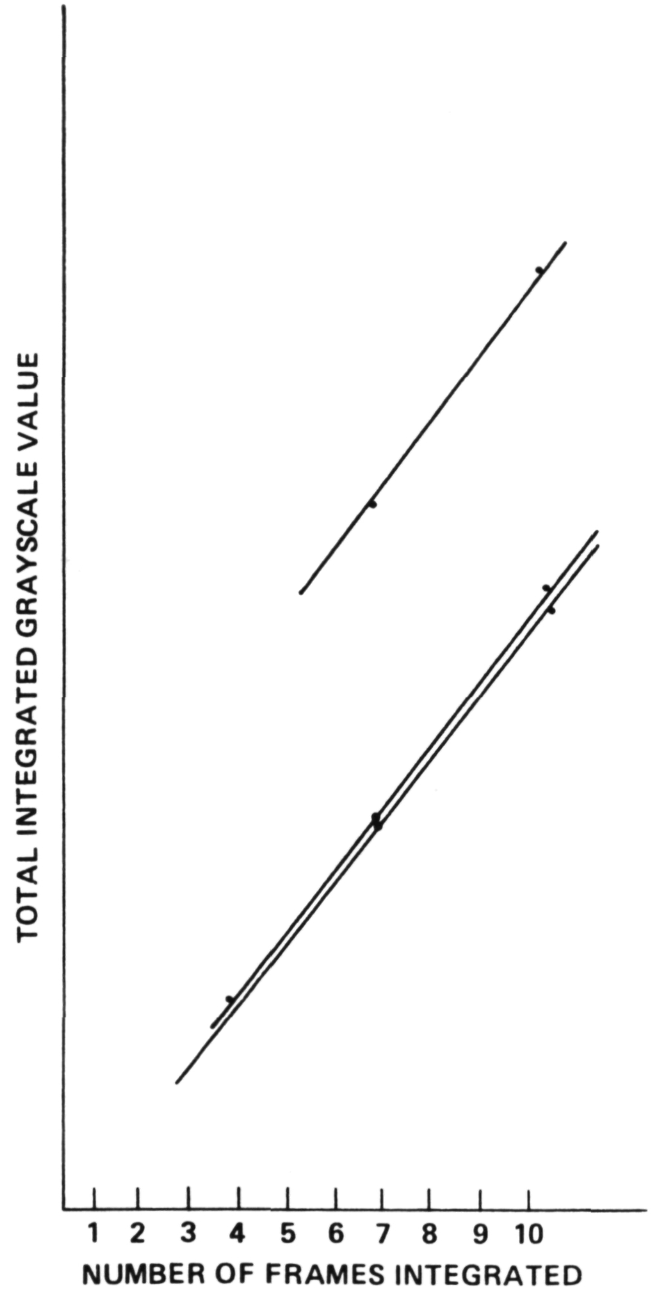

Figure 9. Curves showing the relationship of total integrated grayscale values with increased integration time of the camera for three faint stars.

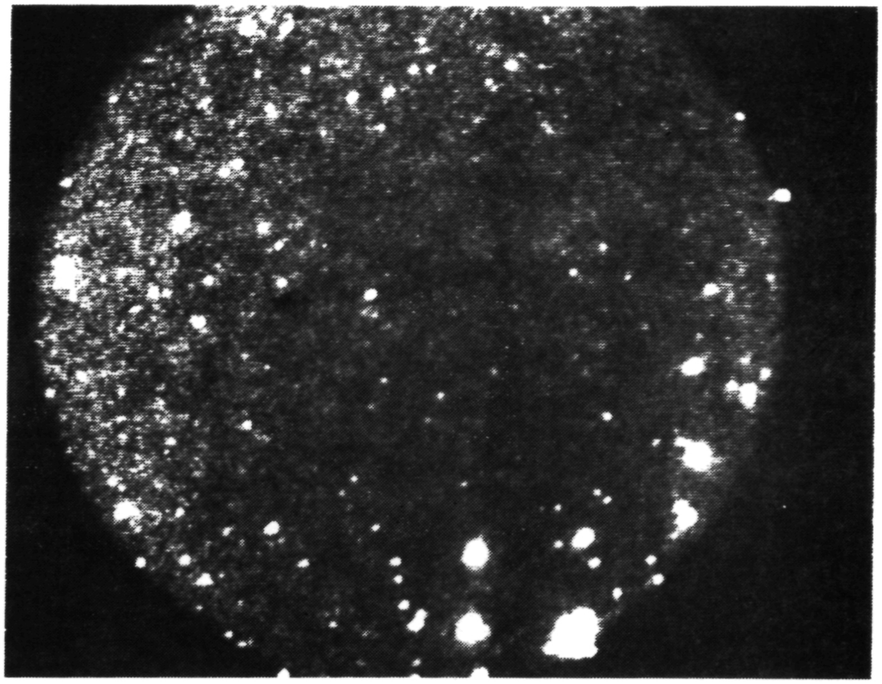

(a)

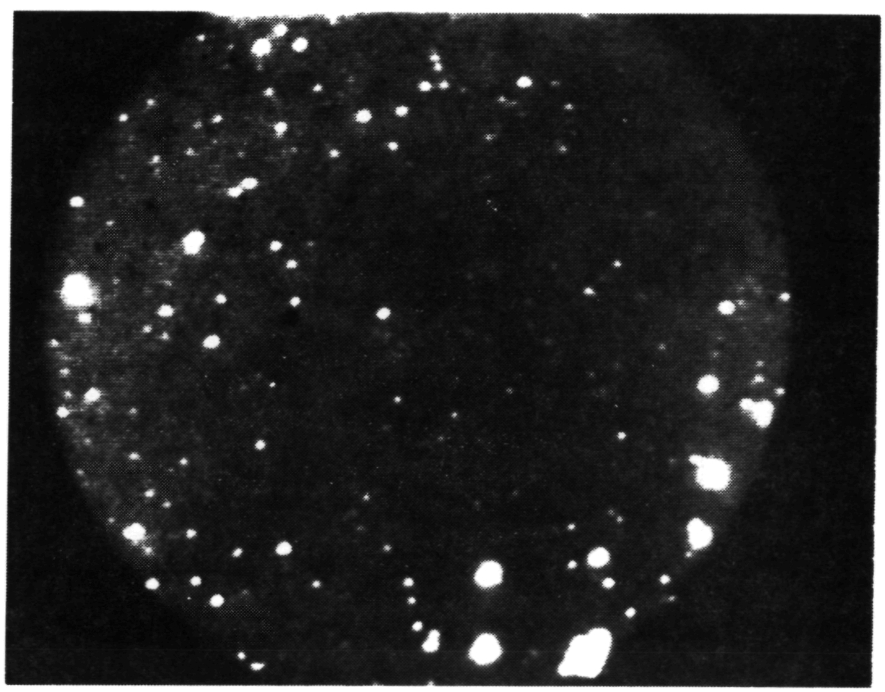

(b)

Figure 10. The effect of averaging frames as seen in (a) an unaveraged frame and (b) a result of 25 averaged frames.

ORIGINAL PAGE IS
OF POOR QUALITY

VI. COMET OBSERVATIONS

Following the observational tests on extended objects and selected starfields, a search was made locally for a known, but faint comet during the moonless periods of the summer months in 1985. During this period only one comet, Comet Giacobini-Zinner (G-Z), was of sufficient brightness to be detected with the Cometary Digital Photometer. However, considerable haze hindered its detection until August 22 when unusually clear weather afforded an excellent opportunity for observation. At this time the comet-Earth distance was 0.49 au, and the comet's heliocentric distance was 1.045 au. The total integrated brightness of the comet, designated 1984e, was reported as approximately 8th magnitude. Observers of the comet had also reported a short tail ranging from a few arcminutes in length to nearly half a degree [11].

Observations of G-Z were made on the morning of August 22 between 0220 and 0420 c.d.t. (0820 and 1020 UT). At that time the comet was positioned in the constellation of Perseus placing it well above the horizon. Figure 11 shows an image obtained at 0418 c.d.t. with the comet at a right ascension of 4^h09^m and a declination of +49 deg. The image was taken from an average of four consecutive frames each integrated for 2.67 s. Adjustment of the camera A/D levels permitted the relatively long integration period without producing saturation effects. The comet appears in the lower right of the figure with a star-like nucleus and a short diffuse tail structure extending upward (westward). North is directed to the left of the image. No star appearing in the field-of-view is listed in the Smithsonian Star Catalog. From a comparison with stars of listed magnitudes appearing in the Palomar Star Charts, it is

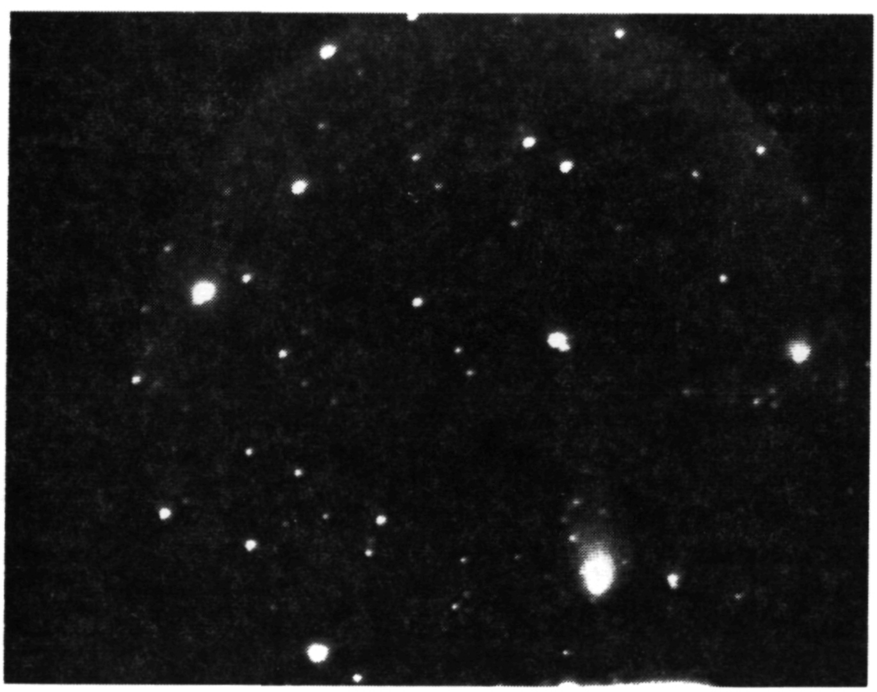

Figure 11. Comet Giacobini-Zinner as seen on August 22, 1985. The comet appears at the lower right of the field-of-view.

apparent that there is no star in the field-of-view brighter than $m_V = 9.0$. This sets an upper limit to the cometary nuclear magnitude which appears somewhat fainter than the brighter stars in Figure 11. However, no absolute photometry was attempted on the image.

Three different representations of the morphology of the comet are presented in Figures 12a-c. Each figure shows a 32 x 64 pixel magnification of the cometary image of Figure 11 corresponding to 3.6 x 7.2 arcmin. The line contour shown in Figure 12 is scaled in arcminutes from the center of the cometary nucleus. Thus roughly 5 arcmin of the tail is displayed in the figures. The smoothing of the isophotes, each representing a grayscale difference of 10, benefitted from the low statistical fluctuations of the background noise. Indeed the standard deviation of the noise amounted only to 3.4 percent of the average background value.

Figures 12b-c show a different form of contouring of the image in Figure 12a. These representations are produced as a result of VIPS processing in which the image is further smoothed and manipulated by a modulus, or mathematical, operation in which the entire 0 to 255 range is repeated over selected brightness intervals. The result is a black and white image similar to that produced by VIPS color contouring. Figures 12b-c differ from each other in the number of contour intervals displayed, the former with four, and the latter, sixteen. The image with fewer contours shows clearly the bending of the dust tail behind the nucleus. The 16-interval image shows more detail and may be compared to the line contours of Figure 12a. The contoured images of the comet may also be compared and contrasted with similar images of G-Z taken in the ultraviolet and infrared spectral region [12,13].

The contouring in Figure 12 shows the detailed structure of the brighter portions of the comet tail to a distance of 5 arcmin. However, traces of the plasma tail can be seen to a greater distance in the intensity line scan of Figure 13. Figure 13 portrays the image intensity (in grayscale levels) as a function of distance, in arcminutes from the nucleus. The scan originates directly above the comet and indicates a detectable tail to a distance of 13 arcmin. This value is commensurate with those reported by observers of G-Z during late August.

VII. SUMMARY AND FUTURE DIRECTIONS

The goal of this project was to develop a digital photometric imaging system capable of observing faint, distant comets. The resulting system can be used either as an adjunct in visual wavelengths to the ongoing infrared cometary observations at MSFC, or on its own to investigate the nature of comets at large heliocentric distances and other questions requiring observations to faint magnitudes. The system is based on an ISEC vidicon camera as the detector supported by a versatile data acquisition system operated on an interactive basis. The ability to view the arriving data and perform real-time analyses permits the optimization of selected images or portions of images for study. The capability to both integrate and frame-average the data results in greater signal-to-noise ratios for faint signals.

Using the camera system attached to a small 8-in. (20 cm) telescope, a limiting magnitude of approximately $m_V = 14$ has been attained over the 40 arcmin field-of-view. Camera controls and integration times must be monitored closely due to the limitations in dynamic range and nonlinearities inherent near saturation levels.

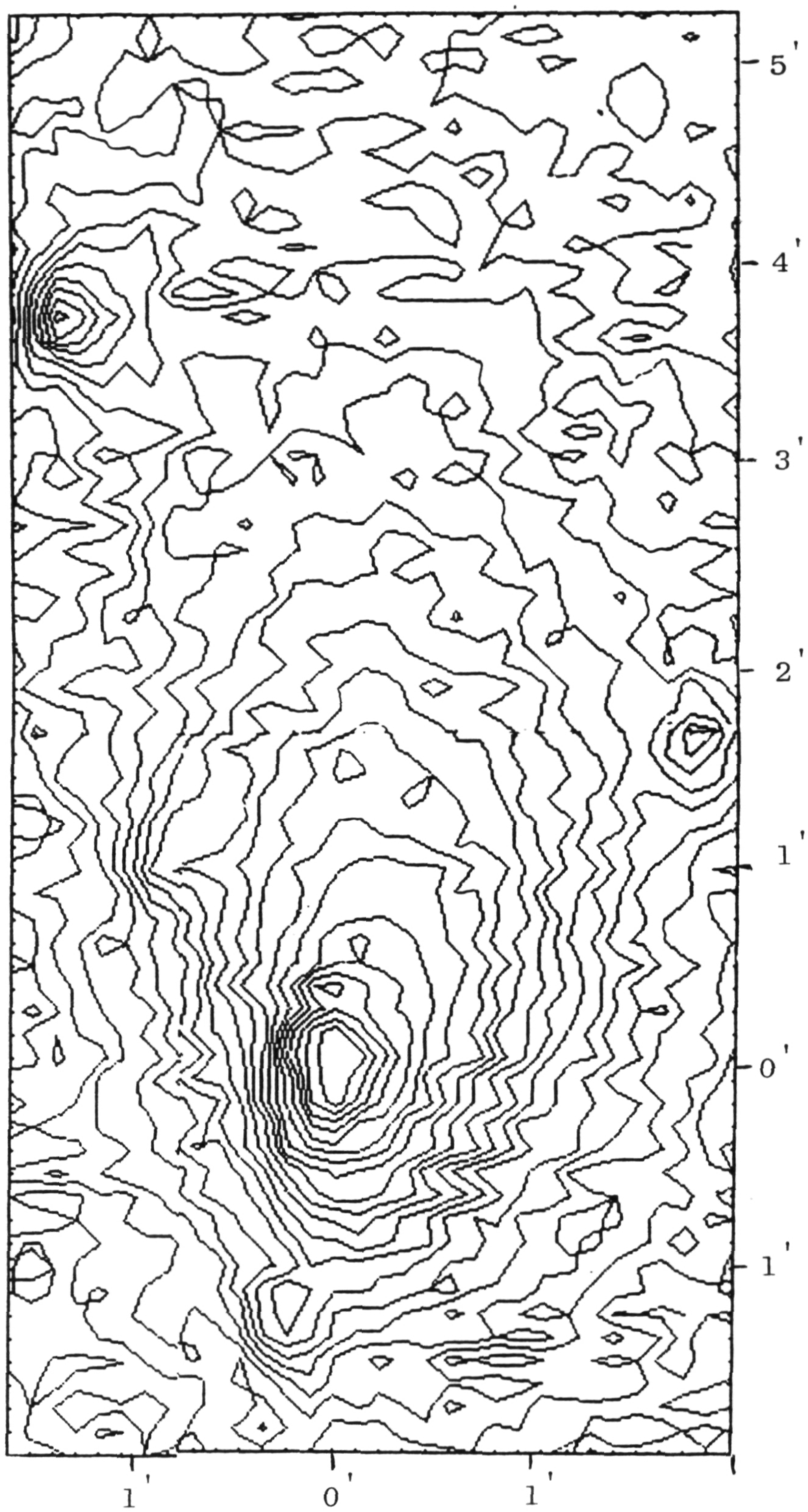

Figure 12. (a) A line contour of Comet Giacobini-Zinner. The image is scaled in arcminutes from the nucleus of the comet. (b) Contour morphology of Comet G-Z using 4 contour intervals and (c) 16 contour intervals.

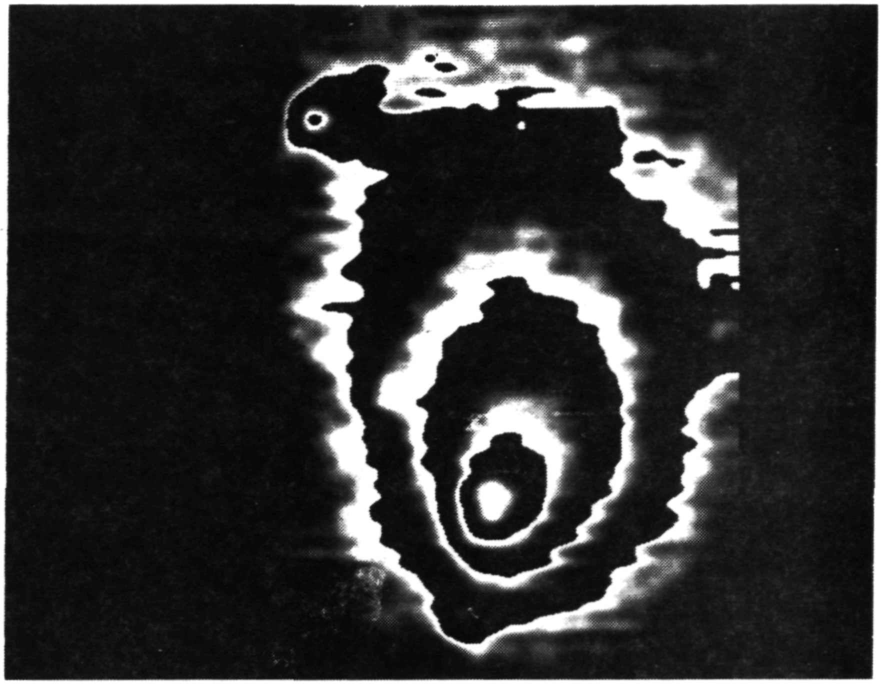

(b)

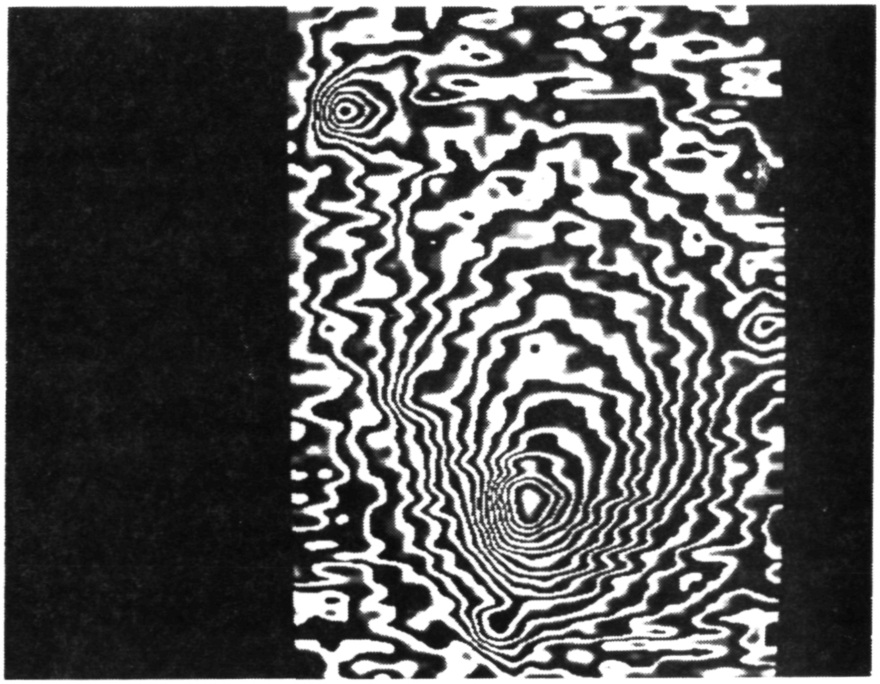

(c)

Figure 12. (Concluded)

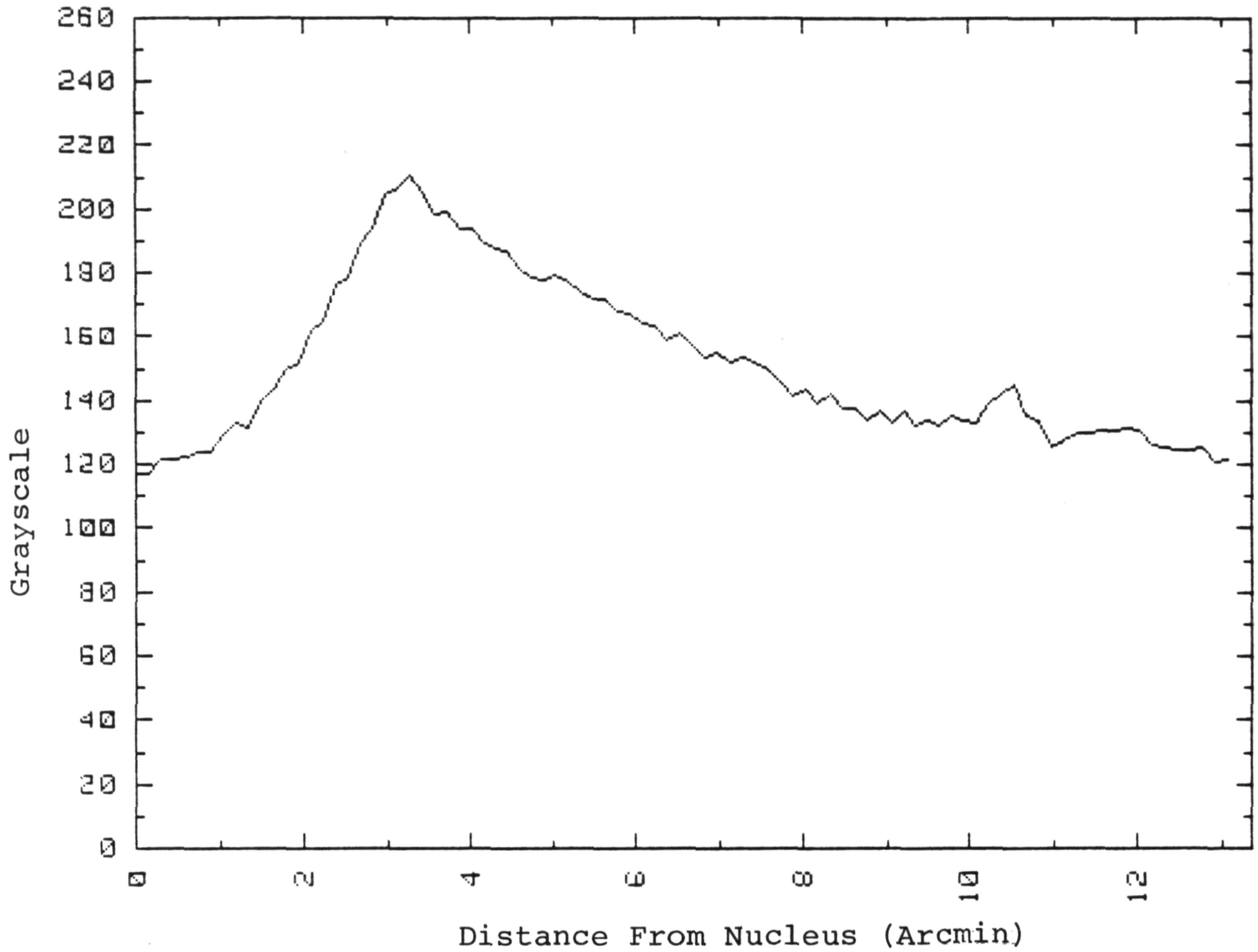

Figure 13. A line scan directly behind the comet showing some tail brightness out to 13 arcmin.

However, these limitations can be overcome without difficulty due to the real-time, interactive nature of the system. Data obtained in the field can be retained through disc storage and further analyzed by a Video Image Processing System. Computer programs designed for digital image analysis allow a broad range of capabilities including black and white and color contouring for morphological studies. Indeed, the digital analysis of the resulting data holds considerable promise in the study of many different aspects of the cometary problem.

Although the CDDF development program ended on August 31, 1985, observations have continued, particularly with the passage of Halley's Comet, a contoured image of which is shown in Figure 14 from observations conducted on December 2, 1985. Observations are planned throughout the spring of 1986, chronicling the outward journey of the comet and noting any changes occurring with increased heliocentric distance. In addition, observations will be conducted of comets of opportunity with magnitudes above detection threshold. The system will be interfaced to larger telescopes at better sites to achieve still fainter magnitudes and faint structural details. The use of the digital photometric imaging system as an adjunct to infrared

cometary studies will also be pursued as part of an RTOP program to provide support to observations in other wavelength regions.

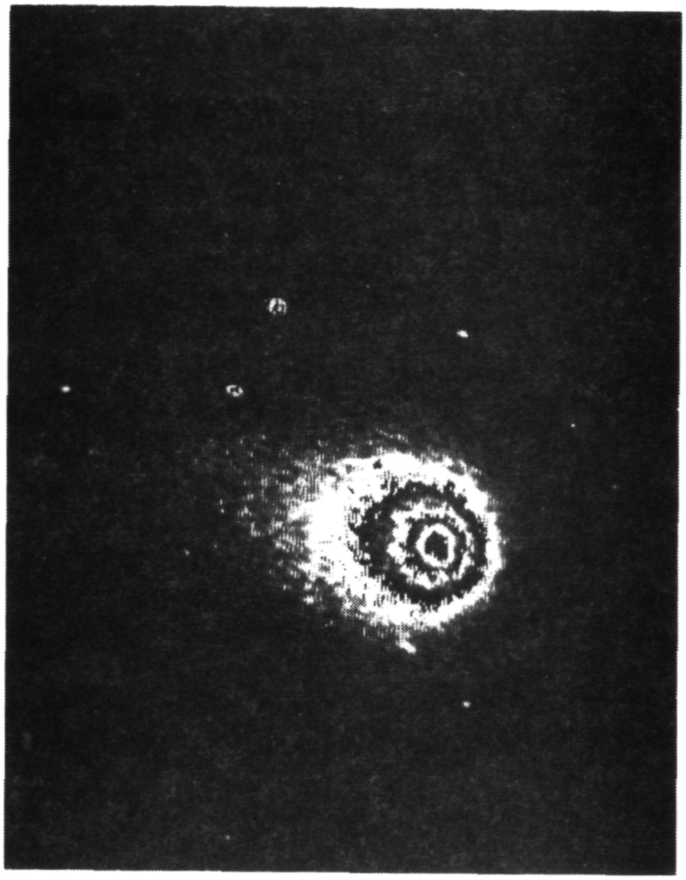

Figure 14. A contoured image of Comet Halley as observed on December 2, 1985.

REFERENCES

1. Duncan, B. J.: A Low Light Level Television System. In Proceedings of the Shuttle-Based Cometary Science Workshop (G. A. Gary and K. S. Clifton, eds.), Marshall Space Flight Center, 1976.

2. Jackson, W. M.: Photochemistry in the Atmospheres of Comets. Molecular Photochemistry, Vol. 4(1), 1972, pp. 135-151.

3. Delsemne, A. H.: Molecular Processes in the Cometary Coma and Tail. In Comet Kohoutek, NASA SP-355 (G. A. Gary, ed.), 1975.

4. Fay, T. D., and Wisniewski, W.: The Light Curve of the Nucleus of Comet d'Arrest. Icarus, Vol. 34, 1978, pp. 1-9.

5. Goetze, G. W.: Secondary Electron Conduction (SEC) and Its Application to Photoelectronic Image Devices. In Advances in Electronics and Electron Physics, Vol. 22A, 1966, pp. 219-227.

6. Beyer, R. R., Green, M., and Goetze, G. W.: Point-Source Imaging with the SEC Target. In Advances in Electronics and Electron Physics, Vol. 22A, 1966, pp. 251-260.

7. Chiu, H. Y., Harris, G. D., Gull, T. R., Maran, S. P., Hobbs, R. W., and Shore, S. N.: Astronomical Observations with an SEC Vidicon System. In Astronomical Observations with Television-Type Sensors, Proceedings of the Symposium, Vancouver, Canada, May 15-17, 1973.

8. Naumann, R. J., and Clifton, K. S.: Mass Influx Obtained from LLLTV Observations of Faint Meteors. NASA TND-6868, 1972.

9. Smithsonian Astrophysical Observatory: Star Catalog. Smithsonian Institution, Washington, D.C., 1966.

10. Burnham, R., Jr.: Burnham's Celestial Handbook. Dover Publications, Inc., New York, NY, 1978.

11. Marsden, B. G.: Periodic Comet Giacobini-Zinner. International Astronomical Union Circular No. 4099, August 28, 1985.

12. Beatty, J. K.: Comet G-Z: The Inside Story. Sky and Telescope, Vol. 70(5), November 1985.

13. Telesco, C. M., Decher, R., Baugher, C., Campins, H., Mozurkewich, D., Thronson, H. A., Cruikshank, D. P., Hammel, H., Larson, S., and Sekanina, Z.: Thermal-Infrared Imaging of Comet Giacobini-Zinner. Submitted to Ap. J. Letters, 1986.

APPROVAL

A DIGITAL IMAGING PHOTOMETRY SYSTEM FOR COMETARY DATA ACQUISITION

Center Director's Discretionary Fund Final Report

By K. S. Clifton, C. M. Benson, and G. A. Gary

The information in this report has been reviewed for technical content. Review of any information concerning Department of Defense or nuclear energy activities or programs has been made by the MSFC Security Classification Officer. This report, in its entirety, has been determined to be unclassified.

E. Tandberg-Hanssen

A. J. DESSLER

Director, Space Science Laboratory

☆U.S. GOVERNMENT PRINTING OFFICE 1986—631-058/20163